Quantum discord for a central two-qubit system coupled to an *XY*-spin-chain environment

Ben-Qiong Liu, Bin Shao,* and Jian Zou
Key Laboratory of Cluster Science of Ministry of Education, and Department of Physics, Beijing Institute of Technology, Beijing 100081, People's Republic of China
(Received 13 September 2010; published 28 December 2010)

We investigate the dynamic behaviors of quantum discord for a central two-qubit system coupled to an *XY*-spin-chain environment. In the weak-coupling regime, we show that the quantum discord for the two central qubits can become minimized rapidly close to the critical point of a quantum phase transition. By considering the two qubits that are initially prepared in the Werner state, we study the evolution of the quantum discord and that of entanglement under the same conditions. Our results imply that entanglement can disappear completely after a finite time, while the quantum discord decreases and tends to be a stable value according to the initial-state parameter for a very-long-time interval. In this sense, the quantum discord is more robust than entanglement for the quantum system exposed to the environment. The relation between the quantum correlations and the classical correlation is also shown for two particular cases.

DOI: 10.1103/PhysRevA.82.062119 PACS number(s): 03.65.Ta, 03.65.Yz, 03.67.Mn

I. INTRODUCTION

Entanglement is a fundamental resource for several applications in quantum information [1] and quantum computation [2] that has attracted considerable interest within various fields of physics. Nowadays, it has been realized that entanglement represents only special kinds of correlations useful for quantum technology, and there exist other nonclassical correlations apart from entanglement that can offer some advantage to these fields. In order to quantify all the nonclassical correlations present in a bipartite system, Ollivier and Zurek [3] introduced the quantum discord, which was defined as the difference between quantum mutual information and classical correlation. For pure entangled states, the quantum discord coincides with the entropy of entanglement. However, the quantumness characterized by quantum discord is different from entanglement and these two measures of correlation are independent, because for some separable states (i.e., pairwise entanglement is absent) the quantum discord can be nonzero. In fact, only zero discord is a necessary condition for strictly classical correlations.

Owing to its theoretical and practical significance, quantum discord has been studied in a number of contexts [4–9], for instance, in a quantum phase transition (QPT) [5,6]. It has been pointed out that the quantum discord increases close to the critical points and it can characterize a QPT. The thermal quantum discord in Heisenberg models has been investigated [6–8], and the results show that it differs in many unexpected ways from thermal entanglement [7], and it may be useful in the experimental detection of critical points for QPTs [6]. Moreover, the concept of quantum discord has been generalized to a continuous variable system for Gaussian states [9]. In particular, some investigations show that quantum discord is more practical than entanglement to describe quantum correlation [10–12], and quantum algorithms based on quantum discord can be more robust than those based on entanglement [13]. Consequently, the quantum discord can be an important resource for the quantum computation task [14].

However, for the realistic quantum systems, they are not closed and their inevitable interactions with the environment lead to the rapid destruction of quantum properties. This decoherence process is regarded as the main obstacle in the development of quantum technology. Recently, there has been an increase in the investigations of the dynamics of quantum discord under the effect of the environment [15–19]. It was shown that [16] the quantum discord was not destroyed by decoherence induced by a noisy environment. Furthermore, both the Markovian [13] and the non-Markovian [17–19] time evolutions of quantum correlations have been investigated, and the results indicate that the quantum discord and entanglement behave differently under the effect of the environment.

In previous studies, the effect of decoherence induced by a correlated environment on the dynamics of the quantum discord has not been investigated. So, in this paper, we present a detailed analysis of the time evolution of quantum discord for a central two-qubit system coupled to an *XY*-spin-chain environment. We calculate the quantum discord and concurrence as the quantifier for entanglement under the same conditions and find remarkable differences between them. The classical correlation is also analyzed.

The paper is organized as follows. In Sec. II, we review the concept of the quantum discord. In Sec. III, we present our physical model and obtain the reduced density matrix of the central two-qubit system. Sec. IV is devoted to the main results of the quantum discord, entanglement, and the classical correlation. Conclusions are presented in Sec. V.

II. QUANTUM DISCORD

We first present a brief review of the quantum discord, which is defined as the difference between two expressions of mutual information extended from the classical to the quantum system.

In classical information theory, the total correlation between two systems A and B, whose state is mathematically represented by a joint probability distribution $p(A,B)$, can be obtained by the mutual information

$$\mathcal{I}(A:B) = H(A) + H(B) - H(A,B), \tag{1}$$

*sbin610@bit.edu.cn

where $H(\cdot) = -\Sigma_j p_j \log_2 p_j$ denotes the Shannon entropy, and p_j represents the probability of an event j relevant to system A or B or the joint system AB. By using the Bayes rule, one can rewrite the mutual information as

$$\mathcal{J}(A:B) = H(A) - H(A|B), \tag{2}$$

where $H(A|B) = H(A,B) - H(B)$ is the classical conditional entropy and it is employed to quantify the ignorance (on average) regarding the value of A when one knows B. In classical information theory, these two expressions are equivalent, but there exists some difference between them in the quantum domain. In order to generalize these expressions to quantum domain, we replace classical probability distributions by the density operator ρ and the Shannon entropy by the von Neumann entropy $S(\rho) = -\mathrm{Tr}(\rho \log_2 \rho)$. In particular, if ρ^{AB} denotes the density operator of a composite bipartite system AB, then $\rho^A = \mathrm{Tr}_B(\rho^{AB})$ and $\rho^B = \mathrm{Tr}_A(\rho^{AB})$ are the reduced density operators for the two subsystems A and B, respectively. Now one can give the quantum versions of Eqs. (1) and (2), respectively:

$$\mathcal{I}(\rho^A:\rho^B) = S(\rho^A) + S(\rho^B) - S(\rho^{AB}), \tag{3}$$

$$\mathcal{J}(\rho^A:\rho^B) = S(\rho^A) - S(\rho^A|\rho^B), \tag{4}$$

where $S(\rho^A|\rho^B)$ is a quantum generalization of the conditional entropy for A and B, and it cannot be directly obtained via the replacement of Shannon entropy by von Neumann entropy. To obtain quantum conditional entropy, we choose projective measurements on B described by a complete set of orthogonal projectors, $\{\hat{P}_j^B\}$, corresponding to outcomes labeled by j. After the measurement, the state of subsystem A changes to $\rho_j^A = [(\hat{I}\otimes\hat{P}_j^B)\rho(\hat{I}\otimes\hat{P}_j^B)]/p_j$, where $p_j = \mathrm{Tr}[(\hat{I}\otimes\hat{P}_j^B)\rho(\hat{I}\otimes\hat{P}_j^B)]$ denotes the probability with respect to the outcome j, and $\hat{I}$ denotes the identity operator for the subsystem A. Therefore, following Eq. (4), one can define the quantum conditional entropy as $S(\rho|\{\hat{P}_j^B\}) = \sum_j p_j S(\rho_j^A)$; consequently, another expression of Eq. (4) based on $\{\hat{P}_j^B\}$ can be given as

$$\mathcal{J}\left(\rho^{AB}:\left\{\hat{P}_j^B\right\}\right) = S(\rho^A) - S\left(\rho^{AB}\middle|\left\{\hat{P}_j^B\right\}\right). \tag{5}$$

Projective measurements on B remove all nonclassical correlations between A and B, and the value of $\mathcal{J}(\rho^{AB}:\{\hat{P}_j^B\})$ depends on the choice of $\{\hat{P}_j^B\}$. According to Henderson and Vedral [20,21], the maximum of $\mathcal{J}(\rho^{AB}:\{\hat{P}_j^B\})$ over all $\{\hat{P}_j^B\}$ can be interpreted as the classical correlation, that is, $\mathcal{C}(\rho^{AB}) = \sup_{\{\hat{P}_j^B\}}\mathcal{J}(\rho^{AB}:\{\hat{P}_j^B\})$. Finally, we get quantum discord as the difference between the total correlations $\mathcal{I}(\rho^A:\rho^B)$ and the classical correlation,

$$\begin{aligned}\mathcal{D}(\rho^{AB}) &= \mathcal{I}(\rho^A:\rho^B) - \mathcal{C}(\rho^{AB}) \\ &= \mathcal{I}(\rho^A:\rho^B) - \sup_{\{\hat{P}_j^B\}}\left[S(\rho^A) - \sum_j p_j S\left(\rho_j^A\right)\right].\end{aligned} \tag{6}$$

Quantum discord can quantify all of the quantum correlations, including entanglement in a bipartite system, such that it is zero only for states with classical correlations and nonzero for states with quantum correlations. For pure states, quantum discord is exactly equal to the entropy of entanglement, as the classical correlation attains its maximum value 1. For general mixed states, the situation is more complicated. Modi *et al.* [22] have discussed the problem of separation of total correlations in a given quantum state into entanglement, classical correlation, and dissonance, which is a similar notion to quantum discord but excludes entanglement. As they presented, entanglement and dissonance belong jointly to quantum discord, but when combined, the two are larger than quantum discord for the W state. In addition, it has been shown that quantum discord is not always larger than entanglement [23]. Therefore, Ali, Rau, and Alber [24] believe that quantum discord is not simply a sum of entanglement and some other nonclassical correlation.

III. PHYSICAL MODEL AND SOLUTION

The total Hamiltonian for the two central spins transversely coupled to an XY-spin-chain environment is composed of two parts [25–27],

$$H = H_I + H_E, \tag{7a}$$

$$H_I = \frac{g}{2}J\left(S_A^z + S_B^z\right)\sum_i^N \sigma_i^z, \tag{7b}$$

$$H_E = J\sum_i^N\left(\frac{1+\gamma}{2}\sigma_i^x\sigma_{i+1}^x + \frac{1-\gamma}{2}\sigma_i^y\sigma_{i+1}^y + \omega\sigma_i^z\right), \tag{7c}$$

where H_I represents the interaction Hamiltonian between the central two-qubit system and the environment, with g denoting their coupling strength, and H_E denotes the self-Hamiltonian of the spin-chain environment. The spin operators $S_{A(B)}^z$ and σ_i^α ($\alpha = x,y,z$) are used to describe the two central qubits and the surrounding chain, respectively. N is the total number of the sites of the chain environment, and the periodic boundary conditions $\sigma_{N+1}^\alpha = \sigma_1^\alpha$ are satisfied. The parameter ω characterizes the strength of the transverse field, and γ defines the degree of anisotropy of the interactions in the xy plane. Hereafter, we take $\hbar = 1$.

Note that $[S_A^z + S_B^z, \sigma_i^\alpha] = 0$, the operator $g(S_A^z + S_B^z)$, which is a conserved quantity, can be treated as a constant corresponding to its eigenvalues in the two-qubit subspace; thus one can rewrite Eq. (7) as

$$H = \sum_{\mu=1}^4 |\phi_\mu\rangle\langle\phi_\mu| \otimes H_E^{(\omega_\mu)}, \tag{8}$$

with $|\phi_\mu\rangle$ ($\mu = 1,2,3,4$) denoting the μth eigenstate of the operator $g(S_A^z + S_B^z)$ relevant to the μth eigenvalue ε_μ. The parameters ω_μ are given by $\omega_\mu = \omega + \varepsilon_\mu$, and the projected Hamiltonian $H_E^{(\omega_\mu)}$ environment is obtained from H_E by replacing ω with ω_μ.

We assume the central two-qubit system and the chain environment are initially uncorrelated with the density operator $\rho^{\mathrm{tot}}(0) = \rho^{AB}(0)\otimes\rho^E(0)$, where $\rho^{AB}(0)$ is the initial density operator of the two central qubits, and $\rho^E(0) = |\varphi_E\rangle\langle\varphi_E|$ and $|\varphi_E\rangle$ are the initial density operator and the initial state of the chain environment, respectively. The subsequent time evolution of the total system is determined by the time evolution operator $\rho^{\mathrm{tot}}(t) = U(t)\rho^{\mathrm{tot}}(0)U(t)^\dagger$. One can obtain the evolved reduced density matrix of the

two central qubits by tracing over the environment, denoted by $\rho^{AB}(t) = \mathrm{Tr}_E[\rho^{\mathrm{tot}}(t)]$. In order to obtain the time evolution operator, we diagonalize the projected Hamiltonian $H_E^{(\omega_\mu)}$ first via a Jordan-Wigner transformation, which maps spins to one-dimensional spinless fermions with creation and annihilation operators $a_n^\dagger$ and a_n, then by using Fourier transforms of the fermionic operators described by $a_n = 1/\sqrt{N}\sum_k d_k e^{i2\pi nk/N}$ with $k = -M, \ldots, M$ and $M = (N-1)/2$ for odd N, and finally by employing a Bogoliubov transformation $\beta_{k,\omega_\mu} = \cos[\theta_k^{(\omega_\mu)}/2]d_k - i\,\sin[\theta_k^{(\omega_\mu)}/2]d_{-k}^\dagger$, with $\theta_k^{(\omega_\mu)} = \arctan[\gamma \sin(2\pi k/N)/(\omega_\mu - \cos 2\pi k/N)]$. The diagonalized form can be written as

$$H_E^{(\omega_\mu)} = \sum_k \Lambda_k^{(\omega_\mu)} \left(\beta_{k,\omega_\mu}^\dagger \beta_{k,\omega_\mu} - \frac{1}{2}\right), \tag{9}$$

where the energy spectrum $\Lambda_k^{(\omega_\mu)}$ reads

$$\Lambda_k^{(\omega_\mu)} = 2\sqrt{\left[\cos\left(\frac{2\pi k}{N}\right) - \omega_\mu\right]^2 + \gamma^2 \sin^2\left(\frac{2\pi k}{N}\right)}. \tag{10}$$

In terms of these notations, one can obtain the time evolution operator for the Hamiltonian (7),

$$U(t) = \sum_{\mu=1}^{4} |\phi_\mu\rangle\langle\phi_\mu| \otimes U_E^{(\omega_\mu)}(t), \tag{11}$$

with $U_E^{(\omega_\mu)}(t) = \exp(-iH_E^{(\omega_\mu)}t)$ representing the projected time evolution operator. Then the reduced density matrix of the two central qubits can be given by the following equation:

$$\rho^{AB}(t) = \langle\varphi_E|U_E^{\dagger(\omega_\nu)}U_E^{(\omega_\mu)}|\varphi_E\rangle\rho^{AB}(0). \tag{12}$$

It can be seen that the spin-chain environment does not affect the diagonal terms of $\rho^{AB}(t)$, because when $\mu = \nu$, the decoherence factor $F(t)_{\mu\nu} = \langle\varphi_E|U_E^{\dagger(\omega_\nu)}U_E^{(\omega_\mu)}|\varphi_E\rangle$ $(\mu,\nu = 1,2,3,4)$ equals 1, and there is no dynamical correlation between the central two-qubit system and the spin-chain environment.

Now we assume that the two central qubits are initially prepared in the Werner state [28],

$$\rho^{AB}(0) = \frac{1-a}{4} I^{AB} + a|\kappa\rangle\langle\kappa|, \tag{13}$$

where $|\kappa\rangle = (|00\rangle + |11\rangle)/\sqrt{2}$ is the maximally entangled state. For $a = 0$, the Werner state becomes totally mixed, and they reduce to the pure state $|\kappa\rangle$ in the case of $a = 1$. According to Eqs. (12) and (13), in the basis spanned by $\{|00\rangle,|11\rangle,|01\rangle,|10\rangle\}$, the reduced density matrix of the two central qubits is given by

$$\rho^{AB}(t) = \frac{1}{2}\begin{pmatrix} \frac{1+a}{2} & aF(t)_{14} \\ aF^*(t)_{41} & \frac{1+a}{2} \end{pmatrix} \oplus \left(\frac{1-a}{4}\right) I_{2\times 2}, \tag{14}$$

where $F(t)_{\mu\nu}$ is the decoherence factor, and $*$ denotes complex conjugation. Now, the key task for us is to obtain the exact expression for the decoherence factor. Let the initial state of the chain environment $|\varphi_E\rangle$ be the ground state of the self-Hamiltonian H_E, denoted by $|G\rangle_\omega$, which can obtained from the ground state of the projected Hamiltonian $H_E^{(\omega_\mu)}$ by the transformation [29,30] $|G\rangle_\omega = \Pi_{k=1}^M(\cos\,\Theta_k^{(\omega_\mu)} + i\,\sin\Theta_k^{(\omega_\mu)}\beta_{k,\omega_\mu}^\dagger\beta_{-k,\omega_\mu}^\dagger)|G\rangle_{\omega_\mu}$ with $\Theta_k^{(\omega_\mu)} = (\theta_k^{(\omega_\mu)} - \theta_k^{(\omega)})/2$. Then the decoherence factor can be written as [25]

$$\begin{aligned} |F(t)_{14}| &= |_\omega\langle G|U_E^{\dagger(\omega_4)}(t)U_E^{(\omega_1)}(t)|G\rangle_\omega| \\ &= \prod_{k>0}\Big[1 + 2\,\sin\left(2\Theta_k^{(\omega_1)}\right)\sin\left(2\Theta_k^{(\omega_4)}\right)\sin\left(\Lambda_k^{(\omega_1)}t\right) \\ &\quad \times \sin\left(\Lambda_k^{(\omega_4)}t\right)\cos\left(\Lambda_k^{(\omega_1)}t - \Lambda_k^{(\omega_4)}t\right) \\ &\quad - 4\sin\left(2\Theta_k^{(\omega_1)}\right)\sin\left(2\Theta_k^{(\omega_4)}\right)\sin^2\left(\Theta_k^{(\omega_1)} - \Theta_k^{(\omega_4)}\right) \\ &\quad \times \sin^2\left(\Lambda_k^{(\omega_1)}t\right)\sin^2\left(\Lambda_k^{(\omega_4)}t\right) \\ &\quad - \sin^2\left(2\Theta_k^{(\omega_1)}\right)\sin^2\left(\Lambda_k^{(\omega_1)}t\right) \\ &\quad - \sin^2\left(2\Theta_k^{(\omega_4)}\right)\sin^2\left(\Lambda_k^{(\omega_4)}t\right)\Big]^{1/2} \\ &\equiv \prod_{k>0} F_k(t). \end{aligned} \tag{15}$$

The decoherence factor can be regarded as the amplitude of the overlap between the two states of the environment under the time evolution operators $U_E^{(\omega_\mu)}$ and $U_E^{(\omega_\nu)}$. When $|F(t)_{14}| \to 0$, it reveals that the quantum coherence between the two central qubits is strongly destroyed by the interaction with the chain environment; when $|F(t)_{14}| \to 1$, the central two-qubit system is slightly affected by the environment. These two particular cases will be discussed in detail in the following section.

IV. CORRELATIONS FOR THE CENTRAL TWO-QUBIT SYSTEM

For the expression of $\rho^{AB}(t)$ in Eq. (14), the condition $S(\rho^A) = S(\rho^B)$ is satisfied, which means that the measurement of classical correlations gives equal values, irrespective of whether the projective measurements are performed on the subsystem A or B. In order to obtain the quantum mutual information of state $\rho^{AB}(t)$, we first calculate its four eigenvalues,

$$\begin{aligned} &\lambda_1 = \frac{1+a}{4} + \frac{a}{2}|F(t)_{14}|, \quad \lambda_2 = \frac{1+a}{4} - \frac{a}{2}|F(t)_{14}|, \\ &\lambda_3 = \frac{1-a}{4}, \quad \lambda_4 = \frac{1-a}{4}. \end{aligned} \tag{16}$$

Then the quantum mutual information in Eq. (3) reads

$$\mathcal{I}(\rho^A : \rho^B) = -(1+a)\log_2\left(\frac{1+a}{4}\right) + \sum_m^4 \lambda_m \log_2 \lambda_m. \tag{17}$$

For the purpose of calculating the classical correlation $\mathcal{C}(\rho^{AB})$, we propose the complete set of orthogonal projectors $\{\hat{P}_j^B = |\delta_j\rangle\langle\delta_j|, j = \|,\perp\}$ for a local measurement performed on the subsystem B, where the two projectors are defined by the orthogonal states

$$|\delta_\|\rangle = \cos\,\xi|0\rangle + e^{i\varsigma}\sin\,\xi|1\rangle, \tag{18a}$$

$$|\delta_\perp\rangle = e^{-i\varsigma}\,\sin\,\xi|0\rangle - \cos\,\xi|1\rangle, \tag{18b}$$

with $\xi \in [0,\pi/2]$ and $\varsigma \in [0,2\pi]$. For these two project measurements, one has $p_{\parallel} = p_{\perp} = 1/2$, thus the reduced density matrices of subsystem A can be obtained as

$$\rho_{\parallel}^{A} = \begin{bmatrix} \frac{1}{2}(1 + a\cos 2\xi) & \frac{\sin 2\xi}{2} a F(t)_{14} e^{i\varsigma} \\ \frac{\sin 2\xi}{2} a F(t)_{14} e^{-i\varsigma} & \frac{1}{2}(1 - a\cos 2\xi) \end{bmatrix}, \tag{19a}$$

$$\rho_{\perp}^{A} = \begin{bmatrix} \frac{1}{2}(1 - a\cos 2\xi) & -\frac{\sin 2\xi}{2} a F(t)_{14} e^{i\varsigma} \\ -\frac{\sin 2\xi}{2} a F(t)_{14} e^{-i\varsigma} & \frac{1}{2}(1 + a\cos 2\xi) \end{bmatrix}. \tag{19b}$$

Subsequently the eigenvalues of the reduced density matrix ρ_j^A can be calculated as

$$\tau_{1,2}^{\parallel} = \tau_{1,2}^{\perp} = \tfrac{1}{2}(1 \pm \chi), \tag{20}$$

with $\chi = \sqrt{a^2(\cos^2 2\xi + |F(t)_{14}|^2 \sin^2 2\xi)}$ and do not depend on the parameter ς. It is straightforward to obtain the quantum conditional entropy $\sum_j p_j S(\rho_j^A) = f(\chi)$, where the function $f(\chi)$ is defined by the following expression for convenience:

$$f(\chi) = -\frac{1-\chi}{2}\log_2\left(\frac{1-\chi}{2}\right) - \frac{1+\chi}{2}\log_2\left(\frac{1+\chi}{2}\right), \tag{21}$$

then the classical correlation is given by

$$\mathcal{C}(\rho^{AB}) = -\frac{1+a}{2}\log_2\left(\frac{1+a}{4}\right) - \min_{\{\hat{P}_j\}}[f(\chi)]. \tag{22}$$

As $f(\chi)$ is monotonically decreasing, we should choose the maximal value of χ for the sake of the minimal value of the function. Obviously, one can see that $\chi \leqslant a\sqrt{(\cos^2 2\xi + \sin^2 2\xi)} = a$ for all the choices of the parameter ξ, because the decoherence factor $|F(t)_{14}|$ is always equal to or less than unity. Finally we have the classical correlation

$$\mathcal{C}(\rho^{AB}) = -\frac{1+a}{2}\log_2\left(\frac{1+a}{4}\right) - f(a). \tag{23}$$

Consequently, the quantum discord can be given by

$$\mathcal{D}(\rho^{AB}) = -\frac{1+a}{2}\log_2\left(\frac{1+a}{4}\right) + \sum_{m}^{4}\lambda_m \log_2 \lambda_m + f(a). \tag{24}$$

It is known that entanglement exhibits very interesting behavior at the QPTs [31], and the quantum critical point can be signaled by measure of entanglement. However, entanglement is only one type of quantum correlation, and there exist nonclassical correlations that cannot be captured by entanglement. It is then natural to ask: What is the behavior of the total amount of quantum correlations close to the critical point of the QTP? To solve the problem, researchers have made some calculations, as we have mentioned before. Here we calculate numerically the exact expression of the quantum discord given by Eq. (24) and analyze the behavior of quantum discord close to the critical point. In Fig. 1(a), quantum discord is plotted as a function of the strength of the transverse field ω and the scaled time Jt in the weak-coupling regime. It is revealed that the quantum discord decreases significantly in a region where the strength of the transverse field approaches the critical point $\omega_c = 1$. At this point, the quantum discord for the two central qubits is minimized with respect to a QPT in the spin-chain environment. Figure 1(b) represents the size dependence of quantum discord for $\omega = \omega_c$ and $g = 0.015$. As expected, the quantum discord for the two central qubits gets minimized in a very short time with respect to a QPT in the XY chain by increasing the size N toward the thermodynamic limit. In fact, entanglement of the two central spins can be used

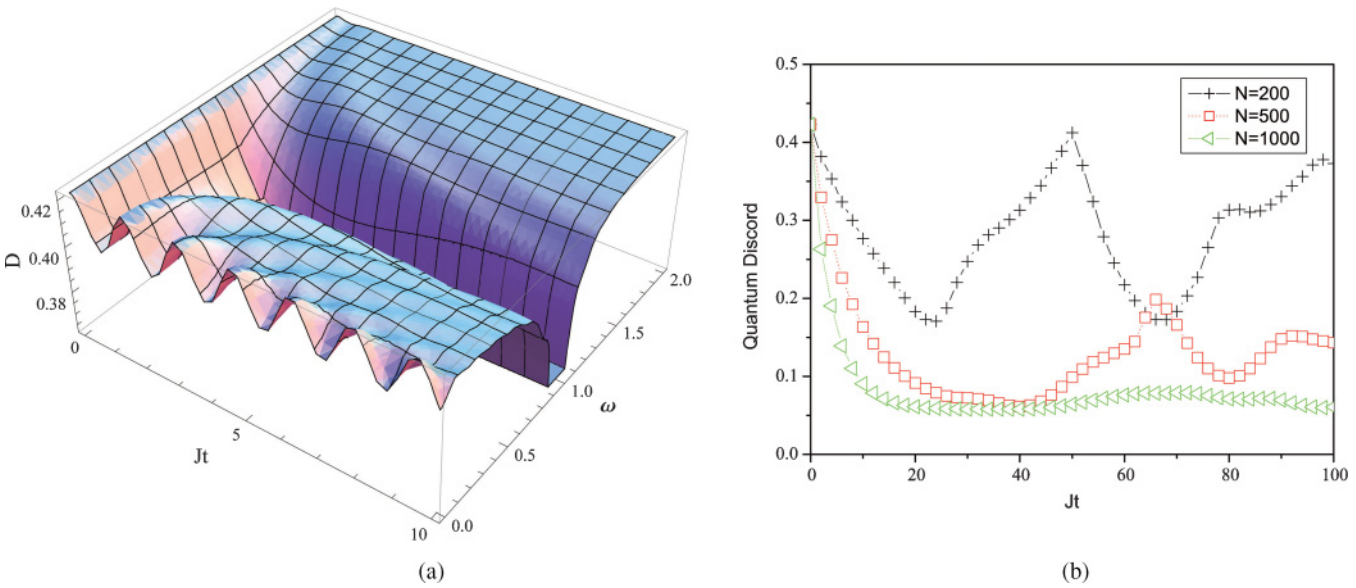

FIG. 1. (Color online) (a) Plot of quantum discord as a function of the strength of the transverse field ω and the scaled time Jt. Other parameters are set as $\gamma = 1$, $g = 0.01$, $a = 0.6$, and $N = 500$. (b) Plot of quantum discord as a function of the scaled time Jt for different sizes of the XY-spin-chain environment: $N = 200$ (cross), $N = 500$ (square), and $N = 1000$ (triangle). Other parameters are set as $\gamma = 1$, $\omega = 1$, $g = 0.015$, and $a = 0.6$.

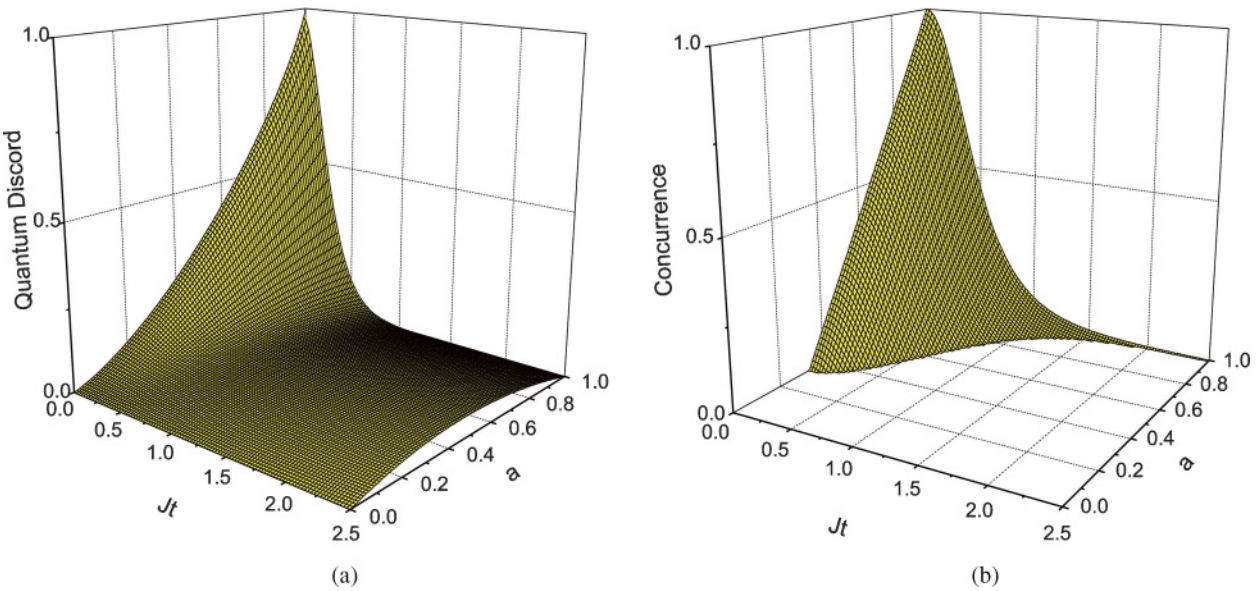

FIG. 2. (Color online) Dynamics of the quantum discord (a) and concurrence (b) as a function of the scaled time Jt and the initial-state parameter a. Other parameters are set as $\gamma = 0.5$, $\omega = 1$, $g = 0.1$, and $N = 500$.

also to determine a QPT in the chain environment. However, because the two qubits are in a Werner state initially, Werner state ρ^{AB} is entangled only when the parameter $a > 1/3$. If the parameter $a \leqslant 1/3$, entanglement is null and cannot characterize a QPT any longer. On the contrary, the quantum discord is still nonzero and can be a useful tool to highlight the critical point of QPT.

In order to study the relation between quantum discord and entanglement, we employ the concurrence [32] as a measure of entanglement. For the Werner state, the concurrence is readily given by

$$C[\rho^{AB}(t)] = \max\left[a\left(|F(t)_{14}| + \tfrac{1}{2}\right) - \tfrac{1}{2}, 0\right]. \qquad (25)$$

In Fig. 2, we plot the dynamics of quantum discord and entanglement for the Werner state as a function of the scaled time Jt and the initial-state parameter a under the same condition. It shows that the quantum discord decays only asymptotically with the variance of the characteristic parameters and tends to remain a stable value in a long-time interval. On the contrary, one can find that concurrence vanishes abruptly in finite time, and this feature has been termed entanglement sudden death (ESD) [33]. When the initial-state parameter lies in the region $a \in [0, 1/3]$, the two central qubits remain unentangled and the concurrence is exactly zero, but we can still have nonzero quantum discord. The clear difference between the behaviors of the quantum discord and entanglement can be found in Fig. 3, where we consider the influence of the anisotropy parameter. One can see that ESD occurs for concurrence, whereas the quantum discord is always positive and tends to be a stable value $\sim$0.06 (according to the initial-state parameter $a = 0.6$ here) as the scaled time Jt continues. The common feature of the dynamics for both of them is a decrease with an increase of the anisotropy parameter.

Let us consider two special cases. In Fig. 4, the quantum discord, classical correlation, and concurrence are plotted as a function of the initial-state parameter a for the cases of $|F(t)|_{14} \to 0$ and $|F(t)|_{14} \to 1$, respectively. Note that a practical environment generally has an infinite size of degrees of freedom, i.e., $N \to \infty$, and the decoherence factor in Eq. (15) may decrease to zero under some reasonable

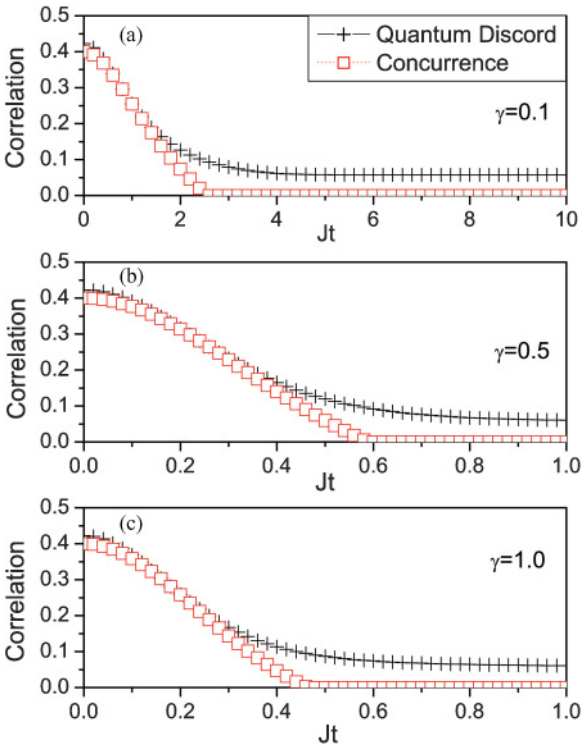

FIG. 3. (Color online) Dynamics of quantum discord (cross) and concurrence (square) as a function of the scaled time Jt for different values of the anisotropy parameter (a) $\gamma = 0.1$, (b) $\gamma = 0.5$, and (c) $\gamma = 1.0$. Other parameters are set as $g = 0.1$, $\omega = 1$, $a = 0.6$, and $N = 500$.

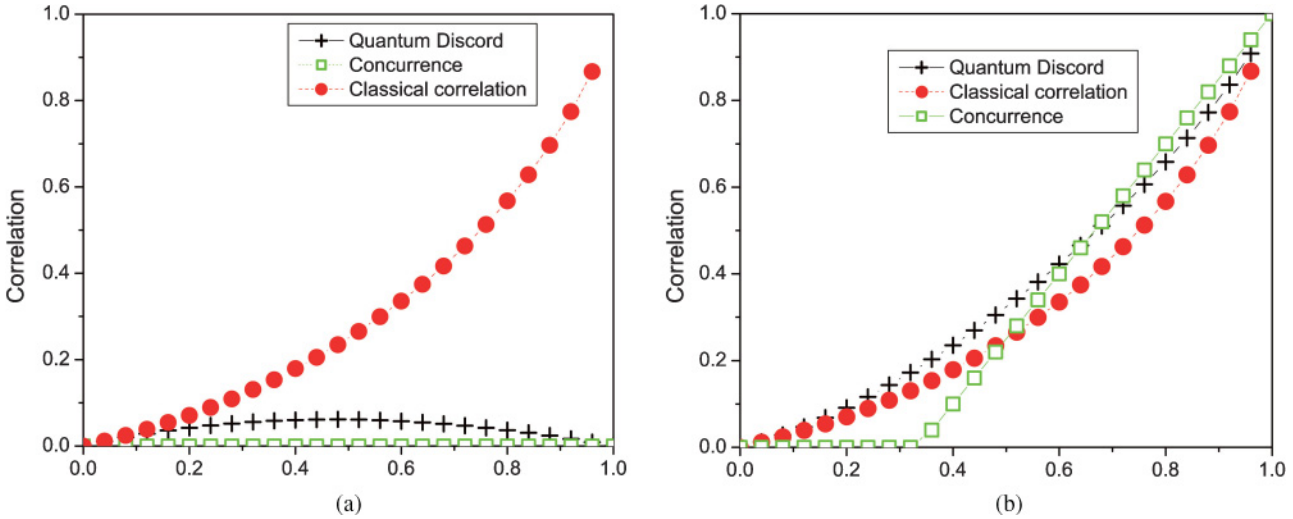

FIG. 4. (Color online) Quantum discord (cross), classical correlation (circle), and concurrence (square) vs the initial-state parameter a (a) for the case of $|F(t)|_{14} \to 0$ and (b) for the case of $|F(t)|_{14} \to 1$.

conditions, because each factor F_k has a norm less than unity. Hence, in the case of $|F(t)_{14}| \to 0$, the quantum discord for the two central qubits in Eq. (24) can be written as

$$\mathcal{D}(\rho^{AB})_{|F(t)_{14}|\to 0} = -\frac{1-a}{2} - \frac{1+a}{2}\log_2\frac{1+a}{2}, \quad (26)$$

but entanglement of the central two qubits is completely destroyed and the concurrence given by Eq. (25) tends to be zero. From Fig. 4(a), we can see that as the initial-state parameter varies from 0 to 1, the classical correlation increases, while the quantum discord is symmetric at approximately $a = 1/2$ and is always less than the classical correlation except for $a = 0$. For the case of $|F(t)|_{14} \to 1$, the interaction between the central two-qubit system and the environment is really weak. Then concurrence of the two central qubits can be written as

$$C[\rho^{AB}(t)]_{|F(t)_{14}|\to 1} = \max\left(\frac{3a-1}{2}, 0\right), \quad (27)$$

and the quantum discord is given by

$$\mathcal{D}(\rho^{AB})_{|F(t)_{14}|\to 1} = a - (1+a)\log_2(1+a) + \frac{1+3a}{4}\log_2 \times (1+3a) + \frac{1-a}{4}\log_2(1-a). \quad (28)$$

As displayed in Fig. 4(b), the quantum discord is always larger than the classical correlation and initially greater than entanglement, but for the range $0.65 < a < 1$, entanglement increases and becomes larger than quantum discord, in agreement with the statement given in Ref. [24].

In what follows, we study the effect of coupling strength on the evolution of the quantum discord; in a like manner we employ concurrence representing entanglement as a comparison. We plot the dynamics of the quantum discord and entanglement as a function of the scaled time Jt with respect to different couplings in Fig. 5. Both the weak-coupling regime and the strong-coupling regime are considered. Under weak coupling ($g = 0.015$), the quantum discord exhibits very complicated oscillations, while entanglement vanishes abruptly within a finite time and remains exactly null for a period of time before its revivals, as was also found for the entanglement sudden death and birth. For the case $g = 0.15$, one can find that the quantum discord decreases monotonously and tends to be a nonzero stable value, but entanglement suddenly falls to zero in a finite time and does not get revived any longer. The decay of both the quantum discord and entanglement can be enhanced by enlarging the coupling strength, as can be seen from the case of $g = 0.15$ to the case of $g = 1.5$. We continue increasing the coupling strength; in particular, for the case $g = 30$, one can see that the evolution of these two measures exhibit some plateaus during the decay process.

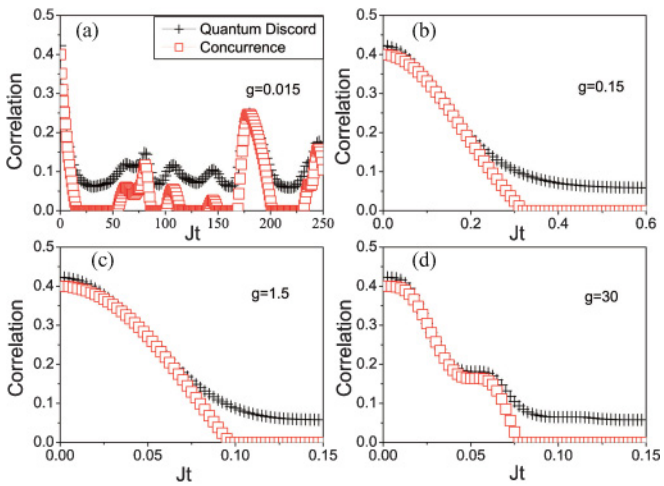

FIG. 5. (Color online) Dynamics of quantum discord (cross) and concurrence (square) as a function of the scaled time Jt for different coupling strengths: (a) $g = 0.015$, (b) $g = 0.15$, (c) $g = 1.5$, and (d) $g = 30$. Other parameters are set as $\gamma = 0.8$, $\omega = 1$, $a = 0.6$, and $N = 500$.

V. CONCLUSION

We have investigated the dynamics of the quantum discord for a central two-qubit system coupled to an XY-spin-chain environment. It has been shown that the quantum discord for the two central qubits gets minimized with respect to the critical point of a QPT in the chain environment. We have calculated the quantum discord and concurrence measuring entanglement in the same range of the physical parameters of interest. It has been found that the decay of both of them can be enhanced by an increase of the anisotropy. For concurrence, the phenomenon of ESD occurs, while for the quantum discord it decreases and tends to be a stable value depending on the initial-state parameter. The difference between these two measures is even more drastic in the region $a \in [0,1/3]$, where the central two-qubit state is initially a separable state. In this case, the interaction between the two central qubits does not lead to the generation of entanglement between them, but really leads to nonzero quantum discord. The relationship between the quantum discord, classical correlation, and entanglement is studied for two particular cases. In addition, the effect of the system-environment coupling strength is also examined.

Our studies indicate that the quantum discord is more robust than entanglement under a decoherence environment, and this advantage may be helpful for the production of quantum states with quantum discord in a long-time interval. Because a stable quantum discord induced by the environment can be obtained, a question arises as to whether the stable quantum discord can become enhanced via controlling the external parameters of some systems. A further study is expected.

ACKNOWLEDGMENT

We acknowledge financial support by the National Natural Science Foundation of China under Grants No. 11075013 and No. 10974016.

[1] V. Vedral, *Introduction to Quantum Information Science* (Oxford University Press, Oxford, UK, 2007).
[2] B. E. Kane, Nature (London) **393**, 133 (1998).
[3] H. Ollivier and W. H. Zurek, Phys. Rev. Lett. **88**, 017901 (2001).
[4] S. Luo, Phys. Rev. A **77**, 042303 (2008); A. Datta, *ibid.* **80**, 052304 (2009); A. Ferraro, L. Aolita, D. Cavalcanti, F. M. Cucchietti, and A. Acín, *ibid.* **81**, 052318 (2010).
[5] R. Dillenschneider, Phys. Rev. B **78**, 224413 (2008); M. S. Sarandy, Phys. Rev. A **80**, 022108 (2009); J. Maziero, H. C. Guzman, L. C. Céleri, M. S. Sarandy, and R. M. Serra, *ibid.* **82**, 012106 (2010).
[6] T. Werlang, C. Trippe, G. A. P. Ribeiro, and Gustavo Rigolin, Phys. Rev. Lett. **105**, 095702 (2010).
[7] T. Werlang and Gustavo Rigolin, Phys. Rev. A **81**, 044101 (2010).
[8] Y. X. Chen and Z. Yin, Commun. Theor. Phys. **54**, 60 (2010).
[9] P. Giorda and M. G. A. Paris, Phys. Rev. Lett. **105**, 020503 (2010); G. Adesso and A. Datta, *ibid.* **105**, 030501 (2010).
[10] A. Datta, S. T. Flammia, and C. M. Caves, Phys. Rev. A **72**, 042316 (2005).
[11] A. Datta, A. Shaji, and C. M. Caves, Phys. Rev. Lett. **100**, 050502 (2008).
[12] B. P. Lanyon, M. Barbieri, M. P. Almeida, and A. G. White, Phys. Rev. Lett. **101**, 200501 (2008).
[13] T. Werlang, S. Souza, F. F. Fanchini, and C. J. Villas Boas, Phys. Rev. A **80**, 024103 (2009).
[14] E. Knill and R. Laflamme, Phys. Rev. Lett. **81**, 5672 (1998).
[15] X.-M. Lu, Z.-J. Xi, Z. Sun, and X. Wang, Quantum Inf. Comput. **10**, 0994 (2010); J.-B. Yuan, L.-M. Kuang, and J.-Q. Liao, J. Phys. B: At. Mol. Opt. Phys. **43**, 165503 (2010).
[16] L. Mazzola, J. Piilo, and S. Maniscalco, Phys. Rev. Lett. **104**, 200401 (2010).
[17] R. Vasile, P. Giorda, S. Olivares, Matteo G. A. Paris, and S. Maniscalco, Phys. Rev. A **82**, 012313 (2010).
[18] B. Wang, Z.-Y Xu, Z.-Q. Chen, and M. Feng, Phys. Rev. A **81**, 014101 (2010).
[19] F. F. Fanchini, T. Werlang, C. A. Brasil, L. G. E. Arruda, and A. O. Caldeira, Phys. Rev. A **81**, 052107 (2010).
[20] L. Henderson and V. Vedral, J. Phys. A **34**, 6899 (2001).
[21] V. Vedral, Phys. Rev. Lett. **90**, 050401 (2003).
[22] K. Modi, T. Paterek, W. Son, V. Vedral, and M. Williamson, Phys. Rev. Lett. **104**, 080501 (2010).
[23] N. Li and S. Luo, Phys. Rev. A **76**, 032327 (2007); S. Luo, *ibid.* **77**, 022301 (2008).
[24] M. Ali, A. R. P. Rau, and G. Alber, Phys. Rev. A **81**, 042105 (2010).
[25] Z.-G. Yuan, P. Zhang, S.-S. Li, Phys. Rev. A **76**, 042118 (2007).
[26] W. W. Cheng and J.-M. Liu, Phys. Rev. A **79**, 052320 (2009).
[27] B.-Q. Liu, B. Shao, and J. Zou, Phys. Rev. A **80**, 062322 (2009).
[28] R. F. Werner, Phys. Rev. A **40**, 4277 (1989).
[29] H. T. Quan, Z. Song, X. F. Liu, P. Zanardi, and C. P. Sun, Phys. Rev. Lett. **96**, 140604 (2006).
[30] Z.-G. Yuan, P. Zhang, and S.-S. Li, Phys. Rev. A **75**, 012102 (2007).
[31] L. Amico, R. Fazio, A. Osterloh, and V. Vedral, Rev. Mod. Phys. **80**, 517 (2008).
[32] W. K. Wootters, Phys. Rev. Lett. **80**, 2245 (1998).
[33] T. Yu and J. H. Eberly, Phys. Rev. Lett. **93**, 140404 (2004).